

Evaluation of 3D Printed Anthropomorphic Head Phantom for Calibration of TLD in Eye Lens Dosimeter

Endarko Endarko^{1*}, Anthonia Wahyu Pitaloka², Amalia Alik Inayah², Fakhruy Rizqy Ramadhan³, Kardianto Kardianto⁴, Betty Rahayuningsih⁵

ABSTRACT

Background: Calibration of Thermo Luminescent Dosimeter (TLD) in eye lens dosimeter requires a standard phantom. The use of anthropomorphic phantoms in calibration needs evaluation.

Objective: This study aimed to analyze the angular response of the TLD on the fabricated 3D anthropomorphic head phantom and Computerized Imaging Reference Systems (CIRS)- Computed Tomography (CT) dose phantom as a standard phantom irradiated with Cs-137 and to compare the absorbed dose and linear attenuation for both phantoms. $H_p(3)$ analysis, conversion coefficient ($h_{pk}(3)$), and calibration factor (CF) are also investigated.

Material and Methods: In this experimental study, the fabricated 3D printed anthropomorphic head phantom was analyzed using polylactic acid (PLA) with the skull and then filled with the artificial brain and cerebrospinal fluid (CSF) as a test phantom. TLD-700H and TLD Reader Harshaw 6600 plus were used to analyze the angular response of Cs-137 radiation and to determine the absorbed dose and linear attenuation coefficient of test and standard phantoms.

Results: The effect of the angle of radiation source towards TLD reading at the anthropomorphic head phantom has a similar value to the standard phantom with a calibration factor ranging from 0.82 to 1. The absorbed dose measurement and the linear attenuation coefficient of the anthropomorphic head phantom with the standard phantom have different values of 2.52 and 3.78%, respectively.

Conclusion: The fabricated 3D printed anthropomorphic head phantom has good potential as an alternative to standard phantoms for TLD calibration in eye lens dosimeter.

Keywords

Calibration; Dosimetry; Phantom; Thermoluminescent Dosimetry; Radiation

Introduction

The International Commission on Radiological Protection (ICRP) report 118 reviewed the upper limit value at 0.5 Gy for the absorbed dose to the eye lens for both acute and protracted exposures [1, 2]. Based on the recommendation, in 2011, ICRP recommended that the dose limit per year for the eye lens amounted to 20 mSv as a 5-year average, with a single-year dose of no more than 50 mSv [3, 4].

According to the IAEA Tec Doc-1731 [5], five medical sectors are

¹PhD, Department of Physics, Institut Teknologi Sepuluh Nopember, Kampus ITS - Sukolilo Surabaya 60111, East Java, Indonesia

²BSc, Department of Physics, Institut Teknologi Sepuluh Nopember, Kampus ITS - Sukolilo Surabaya 60111, East Java, Indonesia

³MSc, Department of Physics, Institut Teknologi Sepuluh Nopember, Kampus ITS - Sukolilo Surabaya 60111, East Java, Indonesia

⁴BSc, Balai Pengamanan Fasilitas Kesehatan Gubeng- Surabaya 60286, East Java, Indonesia

⁵MSc, Balai Pengamanan Fasilitas Kesehatan Gubeng- Surabaya 60286, East Java, Indonesia

*Corresponding author: Endarko Endarko
Department of Physics, Institut Teknologi Sepuluh Nopember, Kampus ITS - Sukolilo Surabaya 60111, East Java, Indonesia
E-mail: endarko@gmail.com

Received: 17 September 2021
Accepted: 20 March 2022

exposed to high radiation doses, especially in the eyes area, for workers, who work close to the patient in radiological intervention procedures, such as in fluoroscopy and nuclear medicine staff for preparing sources or radiopharmaceuticals radiation and equipment, such as Positron Emission Tomography (PET)/Computed Tomography (CT); in addition, the workers involved in manual brachytherapy, CT guided interventional procedures, including biopsy and cyclotron staff are investigated [5]. The best estimate for the dose exposed to the eye lens can be measured using a dosimeter calibration at $H_p(3)$ above the standard phantom as an imitation of a human head [6, 7]. The standard phantom does not represent the anatomy of the human body since the human body is not homogeneous and has various or heterogeneous tissues [8, 9].

Therefore, this work proposed a 3D printed anthropomorphic head phantom for TLD calibration in an eye lens dosimeter. Angular response analysis of TLD-700H for radiation exposure from source Cs-137 was investigated. Moreover, a comparative study of absorbed dose and attenuation coefficient is performed between the standard phantom and 3D printed anthropomorphic head phantom.

Material and Method

Fabrication of 3D Printed Anthropomorphic Head Phantom

In this experimental study, data of patients' skulls in Digital Imaging and Communication in Medicine (DICOM) were taken from embodi3d.com in the stereolithography (STL) file format [10]. The polylactic acid (PLA) filament was used to produce the head phantom using a 3D printer (Creality Ender 5 Plus 3D Printer). The printed head phantom in the study was equipped with an artificial brain and cerebrospinal fluid; the artificial brain was made with a mass, such as an adult human with a 1500 ± 200 g. The composition of the artificial brain was 97% of water (H_2O), 2.5% of agar

($C_{14}H_{24}O_9$), and 0.5% of urea (CH_4N_2O). This combination of materials refers to the ICRP 110 document on the composition of the brain organs [11], and this material was used to obtain solid artificial tissue, identical to human brain tissue, hydrophilic, and non-toxic with high chemical stability. H_2O was heated to a temperature of $75^\circ C$, and agar and urea were then added to H_2O until homogeneous [12].

The artificial cerebrospinal fluid was made using the mixture of NaCl, KCl, $MgCl_2 \cdot 4H_2O$, NaH_2PO_4 , $NaHCO_3$, glucose, and $CaCl_2 \cdot 2H_2O$ with the composition as presented in Table 1. The volume of cerebrospinal fluid in the human head was 120–150 mL, and all ingredients according to the compositions were mixed except for the compound $CaCl_2 \cdot 2H_2O$ in 1 L of pure H_2O at room temperature. The solution was stirred, after all the compounds were mixed in water, the solution was given oxygen gas at 95% for 20 min; oxygen gas was used to dissolve the solution easily and remain at pH 7. The $CaCl_2 \cdot 2H_2O$ compound is added to the solution and stirred until dissolving and mixing. An artificial cerebrospinal fluid was filled into the phantom skull.

Dosemeter

The twelve TLD-700H (7LiF: Mg, Cu, P) and Harshaw TLD Model 6600 plus Automated Reader were used to analyze the angular response of Cs-137 radiation. The calibration and data collection were performed

Table 1: Artificial cerebrospinal fluid composition [13].

Compound	Mass concentration (g/L)
NaCl	6.900
KCl	0.260
$MgCl_2 \cdot 4H_2O$	0.264
NaH_2PO_4	0.120
$NaHCO_3$	2.200
Glucose	1.980
$CaCl_2 \cdot 2H_2O$	0.370

in the Balai Pengamanan Fasilitas Kesehatan (BPFK) Surabaya, Indonesia. Each TLD was calibrated before use, annihilated, heated to a temperature of 250 °C for 10 min with a heating rate of 10 °C/s in a nitrogen environment, and cooled at room temperature naturally to remove the remaining data on the TLD for minimizing reading errors.

The calibration process produced the element correction coefficient (ECC) value on each TLD chip that this ECC was a calibration factor that was compensated for the difference in the sensitivity of each TLD chip [14-17]. Further, ECC was used as a multiplier on the output dose reading so that the reading response of each TLD was proportional to the mean reading response of a group of TLDs or a dosimeter predefined as a recording dosimeter called the golden TLD [17].

Data analysis

In this study, data processing was divided into two: the output dose of TLD reader without normalization by the value of ECC and the output dose of TLD reader normalization by the value of ECC. Eleven TLD-700Hs were used to collect data so that one TLD became background measurement. A background TLD was an unirradiated TLD. When 11 TLDs were irradiated, all TLDs (including back-

ground TLDs) were read with the Harshaw TLD Model 6600 plus Automated Reader. The dose readings produced from the irradiated TLD were reduced with the background TLD readings so that the equivalent dose was obtained from the results of the TLD readings.

Irradiation Data Experiment

The TLD-700H was placed at the head phantom (Figure 1a), with the TLD chip positioned at the center of the forehead. The 3D-printed head phantom was placed on the irradiation desk 2 m apart and set an angle of 0° to the Cs-137 irradiator source. The radiation source used Cs-137 gamma rays with single energy of 0.662 MeV. The TLD was irradiated with an irradiation time of 6.64 min at an air kerma rate of 7.661 mGy/h and repeated three times at the same angle. The TLD was placed in front of the phantom. Irradiation was done at a distance of 2 m perpendicularly, and the dose is calculated according to equation (1) [7]:

$$H_p(3) = KU \times h_{pK} \quad (1)$$

where $H_p(3)$ is the individual equivalent dose at a depth of 3 mm, KU is the value of air kerma at the received radiation distance, and $h_{pK}(3)$ is the conversion coefficient from air kerma to the dose of $H_p(3)$. The same thing was then done at various angles of 30°, 45°, 60°, 90°, 120°, 135°, 150°, and 180°. The radi-

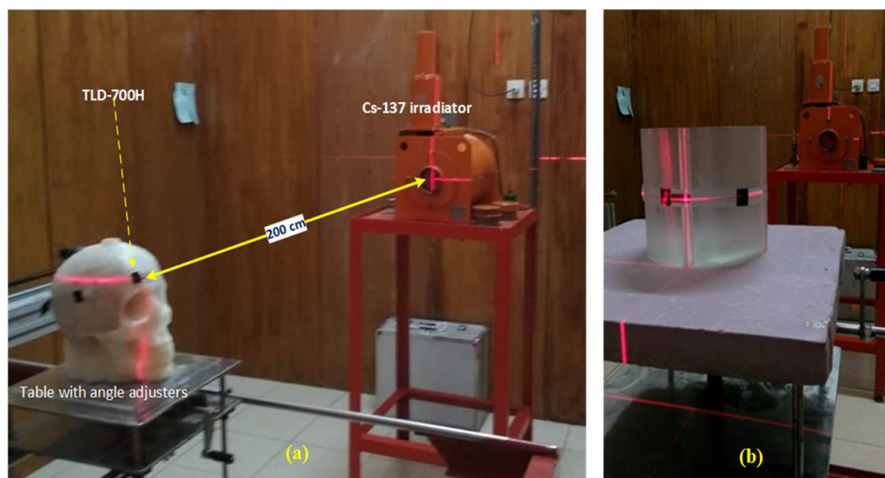


Figure 1: Experimental setup for angular response analysis of Thermoluminescent Dosimetry (TLD)-700H: a) 3D printed head phantom and b) standard phantom.

ation source-detector distance was maintained constant during the measurement with a distance of 2 m for all variations.

The same method was done with a standard phantom with various angles as the 3D printed head phantom (Figure 1b). After the TLD was irradiated, the TLD chip was placed in the holder. The holder filled with the TLD chip was inserted into the TLD reader; the results of the TLD readings were then recorded for the angle of irradiation of the TLD dose readings and subsequently compared with the data collected for the 3D printed head phantom. To determine the absorption dose and linear attenuation coefficient of both 3D printed head phantom and standard phantom. At an angle of 0° , the TLD was placed in the center of the forehead parallel to the back of the head phantom with the same exposure time and repeated three times.

Results

Figure 2 shows the 3D printed anthropomorphic head phantom, consisting of the skull, an artificial brain, and cerebrospinal fluid successfully fabricated and analyzed. CT number in Hounsfield Unit (HU) for 3D printed head phantom was conducted using Philips (Amsterdam, Netherlands) access CT at Siti Khodijah Hospital, Surabaya. The HU values for the skull, artificial brain, and cerebrospinal

fluid were obtained at 130.38 ± 23.43 , 10.09 ± 0.30 , and 10.34 ± 0.38 , respectively.

The dose value of $H_p(3)$ from the 3D printed head phantom was based on PLA, and its percentage of air kerma values is presented in Table 2. The greater the angle of view of the head to the radiation source leads to the smaller the dose read by the TLD. The dose was smaller as the radiation beam angle increased.

Based on Table 1 and equation (1), the conversion coefficient ($h_{pK}(3)$) of a 3D printed head phantom irradiated with Cs-137 is calculated at a distance of 2 m. The results of the calculated $h_{pK}(3)$ is summarized as in Table 3. In 3D printed head phantom and the standard phantom for an angle of 0 to 90° , the conversion coefficient value was still more than 1, i.e. the percentage value of the $H_p(3)$ dose is more than 100%, and the dose received was still higher than the calculation of air kerma.

The calculation of the experimental conversion coefficient using the 3D-printed head phantom provides more accurate results than the standard phantom. The calibration factor can be calculated by comparing the value of the conversion coefficient and the value of $H_p(3)$ measured on the 3D printed head phantom with the standard phantom according to the results reported by Behrens et al., (2012) [7]. The calibration factor was the multiplier value of the TLD dose reading on the 3D

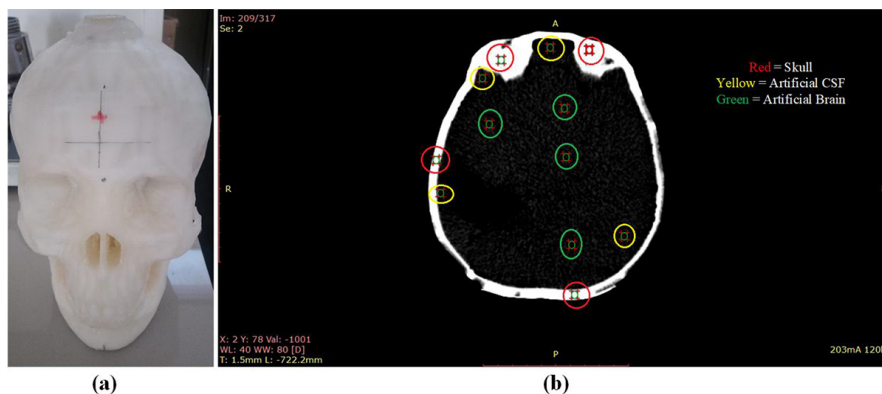


Figure 2: Fabricated 3D printed head phantom: a) view of 3D printed head phantom and b) Computed tomography (CT) image for 3D printed head phantom with selected points of region of interest (ROI) in RadiAnt Dicom viewer software for determining CT number.

Table 2: The dose value of $H_p(3)$ from 3D printed head phantom based on Polylactic Acid (PLA) and its percentage of air kerma values

Angle (°)	ECC without normalization		ECC with normalization	
	Dose (μSv)	Percentage (%)	Dose (μSv)	Percentage (%)
0	943.51 \pm 23.01	111.29	994.48 \pm 12.66	117.30
30	980.73 \pm 23.90	115.68	950.02 \pm 13.18	112.05
45	955.57 \pm 15.23	112.71	947.48 \pm 22.77	111.76
60	1015.01 \pm 25.73	119.72	958.31 \pm 29.33	113.03
90	986.21 \pm 10.01	116.32	1025.83 \pm 63.75	121.00
120	716.00 \pm 17.42	84.45	670.00 \pm 14.85	79.03
135	568.06 \pm 4.79	67.00	566.30 \pm 20.15	66.80
150	478.13 \pm 3.53	56.40	473.83 \pm 22.93	55.89
180	382.42 \pm 5.38	45.11	415.98 \pm 8.36	49.06

ECC: Element Correction Coefficient

Table 3: Value of conversion coefficient, $h_{pK}(3)$ (the conversion coefficient from air kerma to the dose of $H_p(3)$).

Angle (°)	Conversion coefficient (Sv/Gy)		
	3D printed head phantom		Standard Phantom [7]
	ECC without normalization	ECC with normalization	
0	1.11	1.17	1.18
30	1.16	1.12	1.19
45	1.13	1.12	1.20
60	1.20	1.13	1.20
90	1.16	1.21	1.11
120	0.84	0.79	0.69
135	0.67	0.67	0.55
150	0.56	0.56	0.47
180	0.45	0.49	0.41

ECC: Element Correction Coefficient

printed head phantom to match the TLD dose reading results on the phantom standard. Table 4 shows the calibration factor calculation results using equation (2) [18] with a value ranging from 0.82 to 1.07 for both ECC without and with normalization.

$$\text{Calibration Factor (CF)} = \frac{\text{actual dose reading}}{\text{calculated dose reading}} \quad (2)$$

A graph of the angular response of TLD-

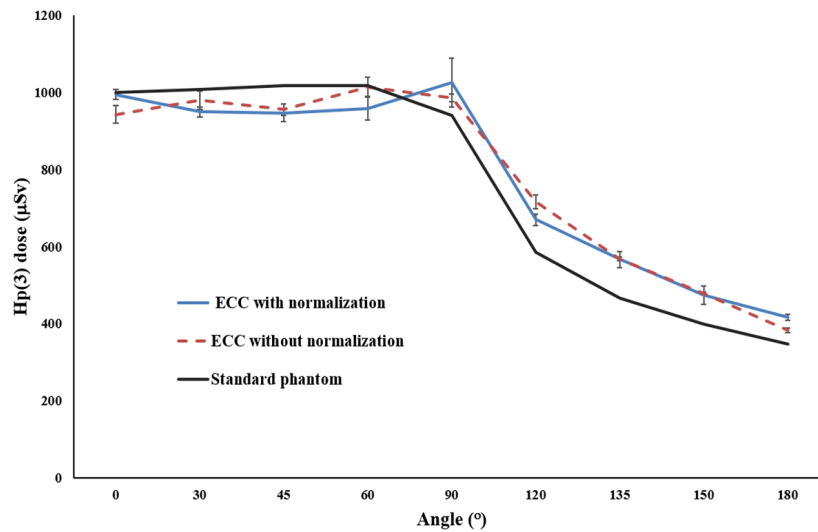
700H toward the irradiation of Cs-137 compared a more precise $H_p(3)$ dose between the 3D printed head phantom and the standard phantom as shown in Figure 3, i.e. the $H_p(3)$ dose was still high at an angle of 0 to 90° then drops; accordingly, the TLD reading is less effective for reading doses above 90° and drastically at an angle of 120°.

Another parameter measured in this study was the absorbed dose to evaluate the ab-

Table 4: Calibration factor for 3D printed head phantom.

Angle (°)	Calibration factor for 3D printed head phantom	
	ECC without normalization	ECC with normalization
0	1.06	1.01
30	1.03	1.06
45	1.06	1.07
60	1.00	1.06
90	0.95	0.92
120	0.82	0.87
135	0.82	0.82
150	0.83	0.84

ECC: Element Correction Coefficient

**Figure 3:** $H_p(3)$ dose as a function of angle for 3D printed head phantom both without and with normalized Element Correction Coefficient (ECC) and standard phantom.

sorbed dose produced by the 3D printed head phantom and the standard phantom. The absorbed dose was calculated using the following equation (3) [19]:

$$H_T = \sum_R w_R D_{T,R} \quad (3)$$

where H_T is an equivalent dose (Sv), w_R is the radiation weighting factor, and $D_{T,R}$ denotes the mean absorbed dose from radiation R in a tissue or organ T (Sv). This study used gamma radiation with a Cs-137 source,

and the value of the weighting factor was 117 for X-ray or gamma radiation, showing that the absorption dose value of a substance was the same as the equivalent dose value ($1 \mu\text{Sv}$ equivalent dose = $1 \mu\text{Gy}$ absorbed dose).

In this study, the average absorbed dose of 3D-printed head phantom without/with normalized ECC was 561.47 ± 5.23 mGy and 626.36 ± 8.32 mGy, respectively. Furthermore, the average absorbed dose of the standard phantom without/with normalized ECC was at 604.78 ± 10.49 mGy and 589.85 ± 21.84 mGy,

respectively.

Meanwhile, the linear attenuation coefficient (μ) for a 3D-printed head phantom and the standard phantom was calculated using the equation as follows (4) [20]:

$$I=I_0 e^{-\mu x} \quad (4)$$

where I was the final dose at a depth of x cm (Gy), I_0 was an initial dose (Gy). The linear attenuation coefficient for 3D printed head phantom both without and with normalized ECC was $5.70 \pm 0.19 \text{ m}^{-1}$ and $5.68 \pm 0.17 \text{ m}^{-1}$, respectively. Furthermore, the standard phantom produced linear attenuation coefficient for both without and with normalized ECC was $5.65 \pm 0.08 \text{ m}^{-1}$ and $5.58 \pm 0.12 \text{ m}^{-1}$, respectively.

Discussion

3D-printed anthropomorphic head phantom must have the equivalent of tissue for a human head. Based on research conducted by Okkalidis et al. the value of HU in the PLA material was 136 [21]. Furthermore, according to Kamalian et al. in 2016, the artificial brain material had an HU value in 20-40 [22]. In this study, the fabricated artificial brains obtained HU values ranging from 10.09 ± 0.30 . When compared to the previous study [22], the artificial brains still had a significant difference due to complicated processes, in which the artificial brain was inserted into the skull. Meanwhile, artificial cerebrospinal fluid had the same value as the research conducted by Osborne et al. with a value of HU at 0–10 [23].

In this study, the data used was $H_p(3)$ with the equivalent dose of the eye lens at a depth of 3 mm [2, 24-26]. The $H_p(3)$ results were obtained from a 3D printed head phantom and standard phantom with various angles of measurement to the Cs-137 radiation source. From Table 2, the greater the angle of view of the head to the radiation source causes the smaller the dose read by the TLD. The dose will be smaller as the radiation beam angle increases, i.e. if the angle of incidence is large, the radiation dose received by radiation workers is

smaller [27].

The conversion coefficient value was used as a multiplier with air kerma so that an equivalent individual dose was obtained at a depth of 3 mm according to $H_p(3)$ [7]. In Table 3, the conversion coefficient value is the same as the percentage value of the $H_p(3)$ dose to air kerma if it is not multiplied by 100%. Accordingly, the conversion coefficient value is the ratio of the dose value read by TLD to the value of air kerma in its irradiation distance [7].

Moreover, the value of the calibration factor summarized in Table 4 shows a number close to 1, i.e. the measurement results in the study using the 3D printed head phantom have a reasonable correlation with the standard phantom measurement reference in the previous studies [7]. The calibration factor is usually generated when calibrating a radiation measuring instrument; the measuring instrument will be better if the calibration factor value is closer to 1. The radiation measuring instrument is feasible if the value of the calibration factor ranges from 0.80 to 1.20 [18]. The calibration factor in this study ranged from 0.82 to 1.0 [7], showing results in this study were still feasible.

Furthermore, for the effect of the angle of irradiation on TLD readings in both the 3D printed head phantom and the standard phantom (Figure 3), a decrease in the dose at an angle of 120° shows that the TLD is less effective for reading doses. Another factor affecting the dose value read TLD is the phantom medium used in the study. When the TLD is directed with an angle bigger than 90° , the radiation beam hits the medium before hitting the TLD. Therefore, the radiation rays hitting the TLD was reduced due to the influence of the medium. However, when viewed from the pattern formed, the two phantoms can provide similar TLD readings after giving TLD to measure the dose of $H_p(3)$.

In addition, the absorbed dose and linear attenuation coefficient for both 3D printed head phantom and standard phantom were performed in this study. The 3D printed head

phantom's absorbed dose against the standard phantom has a different value of 7.16% for ECC without normalized and 6.19% for normalized ECC, showing the different phantom substances and shapes. The standard phantom has a cylindrical shape with a homogeneous PMMA material. Meanwhile, the 3D-printed head phantom is in the form of a heterogeneous skull containing an artificial brain and an artificial brain fluid or cerebrospinal fluid. When compared to the difference in the value of the linear attenuation coefficient of the 3D printed head phantom against the standard phantom, the values obtained are 2.52% and 3.78% for ECC without and with normalization, respectively. The results indicate that the 3D printed phantom has a linear attenuation coefficient similar to the standard phantom. Finally, the 3D printed head phantom has the opportunity to be used as a tool to help measure the dose of $H_p(3)$.

Conclusion

The angular response of TLD-700H on a 3D-printed anthropomorphic head phantom was shown for calibration of TLD in eye lens dosimeter with an irradiation source of Cs-137. 3D-printed anthropomorphic head phantom was fabricated using PLA material as a skull equipped with artificial brain and artificial cerebrospinal fluid. The fabricated 3D-printed anthropomorphic head phantom was successfully used to determine coefficient conversion ($h_{pK}(3)$), $H_p(3)$ dose, absorbed dose, and linear attenuation coefficient. Compared to the standard phantom, the results showed that all parameters have a similar value. Overall, the fabricated 3D-printed anthropomorphic head phantom has the potential used to assess eye lens dosimeters based on the value of $H_p(3)$ dose.

Acknowledgment

Authors thanks the management of Siti Khodijah Hospital and BPFK, Surabaya, Indonesia, who has allowed us to do this study in the CT-Scan and Radiation Protection facilities. The authors gratefully

acknowledge financial support from the Institut Teknologi Sepuluh Nopember for this work, under the project scheme of the Publication Writing and IPR Incentive Program (PPHKI).

Authors' Contribution

E. Endarko was involved in preparing and writing the original draft and reviewing/editing; E. Endarko, AW. Pitaloka, AA. Inayah, FR. Ramadhan were involved in the sample's preparation, investigation, methodology, data collection, and visualization. K. Kardianto and B. Rahayuningsih were involved in the calibration methods and data collection. All the authors read, modified, and approved the final version of the manuscript.

Ethical Approval

The authors have permission to collect data from Badan Pengamanan Fasilitas Kesehatan (BPFK), Surabaya, Jawa Timur, Indonesia.

Conflict of Interest

None

References

1. Stewart FA, Akleyev AV, et al. ICRP publication 118: ICRP statement on tissue reactions and early and late effects of radiation in normal tissues and organs--threshold doses for tissue reactions in a radiation protection context. *Ann ICRP*. 2012;**41**(1-2):1-322. doi: 10.1016/j.icrp.2012.02.001. PubMed PMID: 22925378.
2. Carinou E, Ferrari P, Bjelac OC, Gingaume M, Merce MS, O'Connor U. Eye lens monitoring for interventional radiology personnel: dose-meters, calibration and practical aspects of $H_p(3)$ monitoring. A 2015 review. *J Radiol Prot*. 2015;**35**(3):R17-34. doi: 10.1088/0952-4746/35/3/R17. PubMed PMID: 26343787.
3. International Commission on Radiological Protection (ICRP). Statement on Tissue Reactions [Internet]. 2011. Available from: [https://www.icrp.org/docs/2011 Seoul.pdf](https://www.icrp.org/docs/2011%20Seoul.pdf).
4. Chevallier MA, Rannou A, Villagrasa C, Clairand I. Risk of eye lens radiation exposure for members of the public. *Radiat Prot Dosimetry*. 2016;**168**(1):11-8. doi: 10.1093/rpd/ncv011. PubMed PMID: 25737581.
5. Carinou E. IAEA Tec Doc-1731 'Implications for Occupational Radiation Protection of the New

- Dose Limit for the Lens of the Eye'. *Radiat Prot Dosimetry*. 2016;**171**(4):554-6. doi: 10.1093/rpd/ncw253. PubMed PMID: 27927877.
6. Altaf WJ, Taha MT, Hassan RA, Bahashwan YM. Calibration of TLD in Eye Lens Dosimeter. *J Nucl Tech Appl Sci*. 2017;**5**:87-94.
 7. Behrens R. Air kerma to Hp(3) conversion coefficients for a new cylinder phantom for photon reference radiation qualities. *Radiat Prot Dosimetry*. 2012;**151**(3):450-5. doi: 10.1093/rpd/ncs032. PubMed PMID: 22434922.
 8. International Atomic Energy Agency. Dosimetry in Diagnostic Radiology: An International Code Of Practice. Technical Reports Series No. 457; Vienna: IAEA; 2007.
 9. Wang K, Ho C-C, Zhang C, Wang B. A Review on the 3D Printing of Functional Structures for Medical Phantoms and Regenerated Tissue and Organ Applications. *Engineering*. 2017;**3**(5):653-62. doi: 10.1016/j.eng.2017.05.013.
 10. Embodi3D. Skull and Face [Internet]. 2021 [cited 2021 Apr 26]. Available from: <https://www.embodi3d.com/files/category/12-skull-and-face/>.
 11. Menzel HG, Clement C, DeLuca P. Realistic reference phantoms: an ICRP/ICRU joint effort. *Ann ICRP*. 2009;**39**(2):1-164. doi: 10.1016/j.icrp.2009.09.001. PubMed PMID: 19897132.
 12. Vital KD, Mendes BM, De Sousa Lacerda MA, da Silva TA, Ferreira Fonseca TC. Development of a physical head phantom using of a solid brain equivalent tissue for the calibration of the 18F-FDG internal monitoring system. *Radiat Phys Chem*. 2019;**155**:56-61. doi: 10.1016/j.radphyschem.2018.08.037.
 13. Shiobara R, Ohira T, Doi K, Nishimura M, Kawase T. Development of Artificial Cerebrospinal Fluid: Basic Experiments, and Phase II and III Clinical Trials. *Brain Tumor J Neurol Neurophysiol*. 2013;**4**:173. doi: 10.4172/2155-9562.1000173.
 14. Tawil RA, Pontikos P, Szalanczy A, Velbeck K, Bruml W, Rotunda JE. Thermoluminescent characteristics of new pre-calibrated dosimeters (TLD) in commercially available readers for selected applications. *Nuclear Instruments and Methods in Physics Research Section A: Accelerators, Spectrometers, Detectors and Associated Equipment*. 1994;**353**:411-4. doi: 10.1016/0168-9002(94)91687-X.
 15. Moscovitch M. Personnel Dosimetry Using LiF: Mg, Cu, P. *Radiat Protec Dosim*. 1999;**85**(1-4):49-56. doi: 10.1093/oxfordjournals.rpd.a032904.
 16. Sadeghi M, Sina S, Faghihi R. Investigation of LiF, Mg and Ti (TLD-100) Reproducibility. *J Biomed Phys Eng*. 2015;**5**(4):217-22. PubMed PMID: 26688801. PubMed PMCID: PMC4681467.
 17. Hasabelrasoul HA. Estimation of uncertainty in TLD calibration. Sudan Academy of Sciences (SAS); Sudan: Atomic Energy Council; 2013.
 18. Lewis V, Woods M, Burgess P, Green S, Birmingham R, et al. The Assessment of Uncertainty in Radiological Calibration and Testing. The Assessment of Uncertainty in Radiological Calibration and Testing. United Kingdom: National Physical Laboratory; 2005.
 19. ICRP publication 103. The 2007 Recommendations of the International Commission on Radiological Protection. *Ann ICRP*. 2007;**37**(2-4):1-332. doi: 10.1016/j.icrp.2007.10.003. PubMed PMID: 18082557.
 20. Attix FH. Introduction to Radiological Physics and Radiation Dosimetry. New York: Wiley; 1986.
 21. Okkalidis N, Chatzigeorgiou C, Okkalides D. Assessment of 11 Available Materials With Custom Three-Dimensional-Printing Patterns for the Simulation of Muscle, Fat, and Lung Hounsfield Units in Patient-Specific Phantoms. *J Engand Sci Med*. 2018;**1**(1). doi: 10.1115/1.4038228.
 22. Kamalian S, Lev MH, Gupta R. Computed tomography imaging and angiography - principles. *Handb Clin Neurol*. 2016;**135**:3-20. doi: 10.1016/B978-0-444-53485-9.00001-5. PubMed PMID: 27432657.
 23. Osborne T, Tang C, Sabarwal K, Prakash V. How to interpret an unenhanced CT Brain scan. Part 1: Basic principles of Computed Tomography and relevant neuroanatomy. *South Sudan Medical Journal*. 2016;**9**:67-9.
 24. Bera G, Gellie G, Jamet E, Entine F, Michel X. Eye Lens Radiation Exposure of Workers during Medical Interventional Procedures and Surgery. *Radiat Prot Dosimetry*. 2018;**182**(3):323-8. doi: 10.1093/rpd/ncy068. PubMed PMID: 30590843.
 25. Geber T, Gunnarsson M, Mattsson S. Eye lens dosimetry for interventional procedures - Relation between the absorbed dose to the lens and dose at measurement positions. *Radiat Meas*. 2011;**46**(11):1248-51. doi: 10.1016/j.rad-meas.2011.07.028.
 26. O'Connor U, Gallagher A, Malone L, O'Reilly G. Occupational radiation dose to eyes from

endoscopic retrograde cholangiopancreatography procedures in light of the revised eye lens dose limit from the International Commission on Radiological Protection. *Br J Radiol*. 2013;**86**(1022):20120289. doi: 10.1259/bjr.20120289. PubMed PMID: 23385992. PubMed PMCID: PMC3608047.

27. Nazaroh C, Pardi TB, Irma DR. Observation against Lif: Mg, Cu, P dosimeter which will be used as an eye lens dosimeter for measurement of Hp (3). Nuclear Safety Seminar; Indonesia: IAEA; 2016. Available from: https://inis.iaea.org/collection/NCLCollectionStore/_Public/50/022/50022741.pdf.